ISET Journal of Earthquake Technology, Paper No. 524, Vol. 50, No. 1, March 2013, pp. 27–47

SEISMIC RETROFITTING OF EXISTING STRUCTURES BY TUNED SLOSHING WATER DAMPER: AN EXPERIMENTAL STUDY

Nishant Kishore Rai*, G.R. Reddy**, V. Venkatraj* and P.N. Dubey**

*Directorate of Construction, Services & Estate Management
Department of Atomic Energy, Mumbai-400094
**Bhabha Atomic Research Centre
Department of Atomic Energy, Mumbai-400094

ABSTRACT

The existing medium-height structures (ES) may be retrofitted with tuned sloshing water damper (TSWD) for mitigating increased seismic demands. The performance of TSWD as a response reducing device against vibratory loads is investigated through shake table tests, in coupling with the scaled models (SMs) of ES. The optimum coupling parameters of TSWD with respect to the SMs are obtained through free-vibration tests. Subsequently, the optimally tuned SM-TSWD coupling is subjected to forced sinusoidal vibrations at the resonant frequency. The effectiveness of the proposed retrofitting regime is also tested against ground-motion time histories. The experimental data so obtained is analytically extrapolated for applications to the real-life ES. A response reduction of the order of 25% is predicted for the ES with 1.5% mass ratio. A seismic retrofitting design methodology of 'hardware interactive soft path' for an assured displacement response reduction is devised.

KEYWORDS: Effective Damping Ratio, Effectiveness Ratio, Frequency Ratio, Tuned Sloshing Water Damper

INTRODUCTION

The existing medium-height, non-seismically detailed, reinforced concrete (RC) framed structures are prone to failure due to excessive deformations under seismic loads. The seismic resistance of such structures may be improved by restricting their displacements under dynamic loads within safe limits. This can be achieved by incorporating energy dissipaters, such as tuned liquid dampers (TLDs), in the structural load resisting mechanisms. The commonly used passive dampers, such as hysteretic, viscous, viscoelastic, and self-centering systems, are usually designed to control structural displacements and therefore those end up amplifying the acceleration response of the structures. However, well-designed TLDs are able to reduce both displacements and accelerations in the lightly damped structures (Malekghasemi and Mercan, 2011). For example, shake table tests conducted on the scaled models of a RC framed structure retrofitted with TLDs have shown more than 20% acceleration response reduction under simulated seismic loads (Sharma et al., 2012).

The initial application of TLDs was conceptualised and proposed by W. Froude in 1862, to reduce the rolling motion of ships. This application was then standardized by Frahm (1911). The application of TLDs for ground structures was first proposed by Modi and Welt (1987).

Water is the most economical and commonly used liquid for TLDs. Further, TLDs are classified based on their physical characteristics as tuned liquid column dampers (TLCDs) and tuned sloshing water dampers (TSWDs). A TLCD depends on the inertia of the liquid column in a U-shaped tube to neutralize the dynamic forces acting on the structure. The damping in TLCDs is introduced as a result of the head loss experienced by the liquid column moving through an orifice. A TLCD is unidirectional by design and is well suited for negotiating the wind loads in tall buildings, where the characteristics of the anticipated excitation (i.e., direction and amplitude) can be estimated more accurately (Sakai et al., 1989).

A TSWD has got better applicability potential for the seismic retrofitting of existing structures (ES). Water tanks with designed geometries may be provided as TSWDs to reduce the dynamic response of structures. TSWDs may be constructed in alignment with the principal axes of the ES, thus offering functionality in all possible directions in the horizontal plane (Rai et al., 2011).

A TSWD dissipates energy through liquid boundary layer friction, free surface contamination and wave breaking. Initially, the TSWD parameters were derived through potential flow theory for small excitation amplitudes. Under large excitation amplitudes, TSWDs dissipate a large amount of energy due to their nonlinear behaviour corresponding to wave breaking. Kareem and Sun (1987) developed and validated equations that model a TLD as an equivalent linear tuned mass damper (TMD), where the damper mass is in the form of liquid. The nonlinearity of TSWDs has been addressed by adding empirical amplitude-dependant parameters on well-established TMD linear equations (Sun et al., 1995). An equivalent mass damper system with amplitude-dependent non-linear stiffness and damping has been proposed with the stiffness hardening ratio derived from experimental data (Yu, 1997). A sloshing–slamming model for TSWDs has been proposed by capturing the physics of mass momentum transfer involved in the sloshing phenomenon at high amplitudes (Yalla, 2001). Like the potential flow theory, in all these studies TSWD characteristics under large amplitudes were not captured accurately. However, TSWD–structure interaction was predicted with reasonable accuracy (Hassan, 2010).

The non-linearity of sloshing water in TSWDs, under large excitation amplitudes, has been physically eliminated by incorporating screens normal to the direction of movement. This has resulted in the increased damping ratios of TSWDs, in the absence of wave breaking. Expressions for equivalent linearized damping ratio have been developed and substantiated through shake table experimental observations for the structural response of single-degree-of-freedom (SDOF) structures in coupling with TSWDs (Tait, 2008).

For achieving an effective performance of a vibration absorber it is crucial that the fundamental frequency of the absorber is tuned to the natural frequency of the structure and the damping ratio of its motion is set equal to the optimal value (Warburton, 1981). However, damping induced in TSWDs by the liquid motion is dependent on the vibration amplitudes, which are same as the displacements of the structure. Therefore, for the optimum damping ratio and tuning condition, an accurate assessment of the structural displacements and excitation amplitudes is required.

For response reduction against wind excitations, TSWDs have been installed and their functional usefulness has been established in tall structures (Tamura et al., 1995). However, for the TSWD-retrofitted systems, real-life data required for functionality assurance in the case of seismic events is not available yet. Nevertheless, a simple structural model in coupling with cylindrical TSWDs has been experimented to substantiate the formulations of earlier researchers and the same formulae have been proposed for the seismic retrofitting of an existing structure (Reddy et al., 2008).

This paper proposes to use the laboratory data, which has been generated through simulated verification testing on the scaled models (SMs) having dynamic similitude with ES (Langhaar, 1951), for assured functionality of the TSWD systems at the required instant of time. The similitude in terms of frequency, damping ratio, geometry, aspect ratios, number of structural elements and joints is established between ES and SMs. A bare SM is considered representative of the unretrofitted ES and a coupled SM-TSWD represents the retrofitted ES. The TSWDs actually proposed to be installed on the ES are tested on shake table, in coupling with the SMs.

Unlike the previous studies wherein the parameters of the TSWDs alone were studied, this paper focusses on the coupled behaviour of the TSWDs and structures and thus is an attempt to bridge the gap between the theoretical studies and the real-life data. The main objectives of this paper are as follows:

1. Study of the dynamic characteristics of a coupled SM-TSWD system through shake table experiments and comparison of the TSWD parameters thus determined with those obtained by the previous researchers by experimentation on TSWDs alone (Yu, 1997; Yalla, 2001).
2. Experimental verification of the effectiveness of TSWD-based retrofitting systems on SMs for displacement response reduction.
3. Development and illustration of a retrofitting methodology with TSWDs for real-life ES and substantiation of its suitability with respect to the assured performance at the required instant of time. This methodology is explained with the example of an existing four-story building, for achieving a predetermined displacement response reduction by installing TSWDs.

The methodology proposed in this paper may be applied to most of the medium-height, 4–10 story existing structures. The TSWDs may be integrated with the plumbing systems of the ES to serve for the thermal storage and fire fighting requirements. This retrofitting system has the advantages of minimal interference with the occupancy and an all time performance assurance at almost zero-maintenance cost (Rai et al., 2010).

STATE OF EXISTING STRUCTURES AND RETROFITTING STRATEGY

The existing medium-height structures are made of RC frames with masonry infills. The quality of masonry is generally poor by structural considerations, and hence the masonry may give way at very small deformations under the dynamic loads. The failure of masonry leads to stiffness loss and catastrophic effects for structures during earthquakes. Thus, the retrofitting strategy is governed by the purpose of restricting the structural displacements within the safety limits in a seismic eventuality. The structures are designed with the working stress method and those possess damping ratios in the range of 2–3%. The retrofitting approach of coupling TSWDs with ES is thus considered to be appropriate.

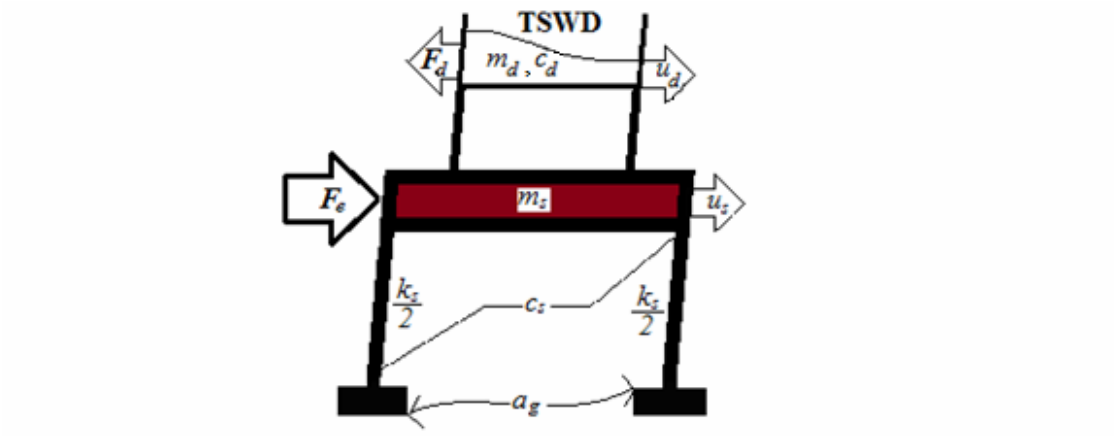

Fig. 1 Structure with TSWD

The dynamic structural response of ES is dependent on frequency ω_s and damping ratio ξ_s. The structure is assumed as an SDOF system corresponding to its first mode, where major part of its mass participates during the vibrations. The structural deformation of this SDOF is governed by its dynamic magnification factor $\mathrm{DMF_o}$ given as

$$\mathrm{DMF_o} = \frac{1}{2\xi_s} \tag{1}$$

The ES are retrofitted by rigidly attaching TSWD of mass m_d, frequency ω_d and damping ratio ξ_d to them.

ES modelled as SDOF systems and retrofitted with TSWDs may be considered as linear 2-DOF systems (see Figure 1). The concept of dynamic magnification factor DMF_r for an undamped structure coupled with a damper was given by Den Hartog (1962). This concept has been subsequently extended to real-life structures with some damping. The dynamic magnification factor for the 2-DOF system under a harmonic excitation is derived as (Yu, 1997)

$$\mathrm{DMF}_r = \frac{1}{\sqrt{\mathrm{RE}^2 + \mathrm{IM}^2}} \tag{2a}$$

with

$$\mathrm{RE} = 1 - \beta^2 - \mu\beta^2 \frac{f^2\left\{f^2 - \beta^2 + \left(2\xi_d\beta\right)^2\right\}}{\left(f^2 - \beta^2\right)^2 + \left(2f\xi_d\beta\right)^2} \tag{2b}$$

$$\mathrm{IM} = 2\xi_s\beta + \frac{2\mu f\xi_d\beta^5}{\left(f^2 - \beta^2\right)^2 + \left(2f\xi_d\beta\right)^2} \tag{2c}$$

Here, $\beta = \omega_e/\omega_s$ is the frequency ratio, $\mu = m_d/m_s$ is the mass ratio, $f = \omega_d/\omega_s$ is the tuning ratio, and ω_e is the frequency of excitation.

The equivalent damping ratio ξ_e of the coupled structure may be given as

$$\xi_e = \frac{1}{2 * \mathrm{DMF}_r} \tag{3}$$

For the condition of $f = 1$ and $\beta = 1$, Equation (2a) leads to (Connor, 2003)

$$\xi_e = \frac{\mu}{2}\sqrt{1+\left(\frac{2\xi_s}{\mu}+\frac{1}{2\xi_d}\right)^2} \tag{4}$$

It is evident from this equation that the equivalent damping ratio of the retrofitted structure depends on f, μ, β, ξ_s and ξ_d. Any modification of the dynamic properties of ES is tedious, inconvenient and obstructive, and hence, is considered beyond the scope of this paper. The only controllable tuning parameters are ω_d, ξ_d, and μ. The ES and TSWD are considered to be tuned if $\omega_d \approx \omega_s$. In this condition, under the dynamic loading, the sloshing mass of water in the TSWD will resonate with the motion of the SDOF system, and a part of the seismic energy imparted on this system will be dissipated. The energy dissipation will result in a reduced response of the coupled structure.

The required damping mass M_d for effective retrofitting may not be small enough to be accommodated in a single TSWD. Thus, N number of TSWDs may be required such that

$$M_d = Nm_d \tag{5}$$

The DMF_o of the bare ES is maximum when the frequency content of the ground motion is same as that of the ES, i.e., at $\beta = 1$ (or, $\omega_e = \omega_s$). The ES have to be retrofitted with TSWDs for such an eventuality.

TUNED SLOSHING WATER DAMPERS

A TSWD consists of a rigid vessel holding a given mass of water and rigidly attached with the structure (see Figure 2). The water in the tank is tuned with the primary frequency of the host structure. The sloshing mass of water resonates with the motion of the host structure. The energy dissipation is caused by the sloshing of water contained in the vessel. Some part of the seismic energy imparted to the structure is dissipated by the sloshing motion of water, thereby modifying the resultant structural response to be within acceptable limits.

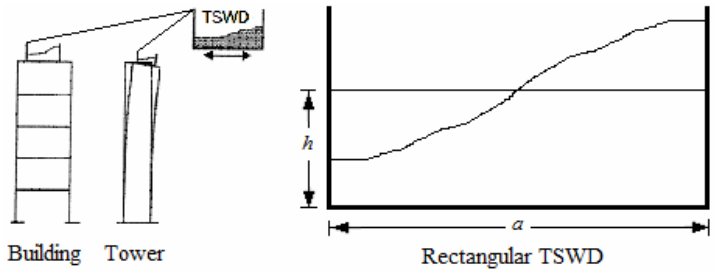

Fig. 2 TSWD on a structure

The linear sloshing frequency of liquid, ω_n, in a TSWD, on the basis of linear wave theory, is given as (Abramson, 1966)

$$\omega_n^2 = \frac{g(2n-1)\pi \tanh(2n-1)\pi r}{a} \tag{6}$$

The nonlinearity of the sloshing liquid frequency has been captured by the following empirical relations (Yu, 1997):

$$\omega_d = \omega_n \left\{1.037\left(A_e/a\right)^{0.0035}\right\} \text{ for } A_e < 3\% \text{ of the tank dimension } a \tag{7a}$$

$$\omega_d = \omega_n \left\{1.59\left(A_e/a\right)^{0.125}\right\} \text{ for } A_e > 3\% \text{ of the tank dimension } a \tag{7b}$$

The mass of sloshing water, m_d, is given by the potential flow theory as (Graham and Rodriguez, 1952)

$$m_d = M \frac{8\tanh\left\{\left(2n-1\right)\pi r\right\}}{r\pi^3\left(2n-1\right)^3} \tag{8}$$

For the seismic design of rectangular water tanks, the sloshing mass is designated as convective mass and this equation is then simplified for the fundamental mode of vibration as (Housner, 1963)

$$m_d = M \frac{0.83\tanh 3.2r}{3.2r} \tag{9}$$

where n is the mode number for the sloshing mode and is equal to 1 for the fundamental mode; M is the total mass of liquid in the tank; g is the gravitational acceleration; h is the depth of liquid in the tank; a is the tank dimension in the direction of vibration; $r = h/a$; and A_e is the vibration amplitude of the TSWD (and is equal to the structural displacement at the TSWD location).

The damping ratio ξ_d of TSWD is a function of A_e/a and this ratio thus depends on the amplitude of excitation and tank dimension. Yalla (2001) and Yu (1997) have respectively proposed the empirical relationships for this ratio as

$$\xi_d = 1.78\left(A_e/a\right)^{0.68} \tag{10a}$$

$$\xi_d = 0.5\left(A_e/a\right)^{0.35} \tag{10b}$$

The mean values of the damping ratio obtained from these equations are shown in Figure 3 and are considered in the present study for the initial calculations.

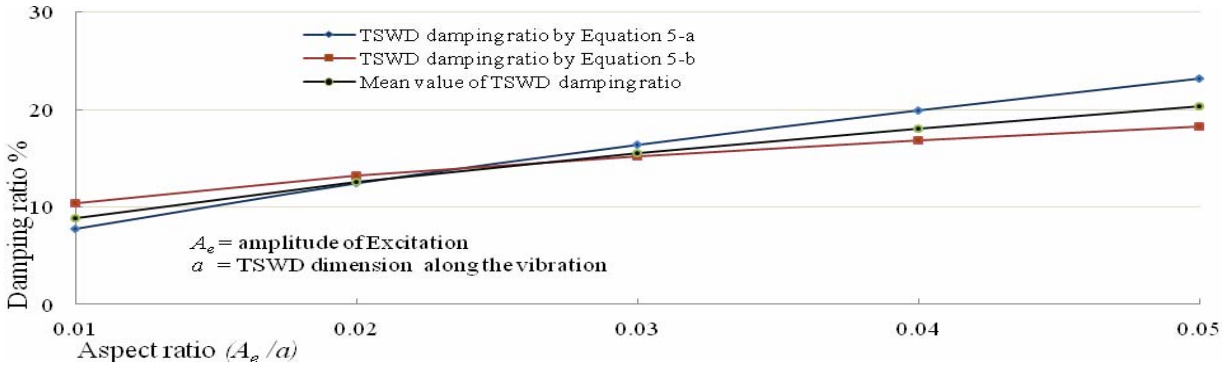

Fig. 3 Variations of the damping ratio of TSWD with the amplitude of excitation

EFFECTIVENESS OF RETROFITTING SYSTEM

The effectiveness of a TSWD retrofitting system is expressed by a non-dimensional parameter. This parameter, called as effectiveness ratio E, denotes the percentage reduction in structural displacement due to the application of retrofitting measure as (Rai et al., 2011)

$$E = \left\{1-\left(D_p/D_m\right)\right\}\times 100 \text{ or } E = \left[1-\left\{\text{DMF}_r/\text{DMF}_o\right\}\right]\times 100 \tag{11}$$

For the combinations of TSWDs with ES, the effectiveness of TSWDs depends on their tuning with ES and increases with an increase in the mass ratio μ.

RETROFITTING METHODOLOGY

The above-described concept of response control may be applied directly to ES to perform with all the advantages of TSWDs. A 'hardware interactive soft path' methodology is proposed in this paper for the assured retrofitting performance. The reduced scaled model (SM) of the existing structure together with the (full-size) proposed TSWDs is the hardware processed through the analytical path for the design of the desired retrofitting regime. The proposed step-by-step methodology is as follows:

- Step 1: The structure to be retrofitted is idealized for a theoretical analysis. The damping ratio of the structure is assumed with due engineering justification. The reference values of dynamic properties, such as first-mode frequency ω_s, damping ratio ξ_s, and maximum displacement D_m, under a particular dynamic excitation are determined analytically. Depending on the structural assessment, the values of maximum permissible displacement D_p and targeted effectiveness E are fixed.
- Step 2: Based on the analysis of the structure, the dimensions of TSWDs are obtained for the frequency $\omega_d = \omega_s$ and the amplitude of excitation $A_e = D_p$ through Equations (6), (7a) and (7b). The damping ratio ξ_d of the TSWDs is obtained from Figure 3.
- Step 3: A physical SM of the structure matching with the experimental resources available is constructed. The SM should have same dimensional aspect ratios with respect to the plan, elevation and floor height as well as the same number of structural members and joints as those in the structure.
- Step 4: The SM is subjected to free vibrations for determining its fundamental frequency. The floorwise distribution of loads is fine-tuned in such a way that $\omega_{es} = \omega_{sm}$. The load distribution on SM is kept similar to that on the structure, and the symmetry of loading about the axis of symmetry is maintained.
- Step 5: A virtual model of SM, designated as VSM, is developed such that SM is simlar to VSM. The VSM is analyzed and its frequency is determined. It is ensured that the first-mode frequency of the VSM becomes equal to the fundamental frequency of the SM. For this, the material and sectional properties of the members in VSM are suitably adjusted. Thus, the first-mode frequency of the structure is equal to the fundamental frequency of the SM and that in turn is equal to the first-mode frequency of the VSM (i.e., $\omega_s = \omega_{es} = \omega_{sm} = \omega_{vsm}$).
- Step 6: The TSWDs are constructed as proposed in Step 2 and are coupled with the SM by mounting those rigidly at the location of $D_p = A_e$. The dimensions of TSWDs are experimentally fine-tuned for the pre-determined depth of water (as proposed in Step 2), under free-vibration tests, by varying the length of TSWDs along the direction of vibration. The length of TSWDs at which the fastest decay of the SM-TSWDs coupling vibration occurs is considered as optimum for the mutual tuning of SM and TSWDs.
- Step 7: The SM without water in the TSWDs, designated as bare SM, is subjected to a forced sinusoidal excitation of the resonant frequency through shake table. The bare SM is subjected to a range of excitation amplitudes at its base, and displacements at the base of TSWDs (i.e., at the location of $D_p = A_e$) are recorded through a laser displacement sensor. The damping ratio of the bare SM, ξ_s, is determined by Equation (1). The VSM is also analyzed with the experimentally obtained values of ξ_s for the sinusoidal excitations of similar amplitudes. The analytically obtained displacements for the VSM should match the experimental observations on the SM. In the case of major discrepancies, Steps 3, 4 and 5 are repeated with suitable modifications in the load distribution of SM and input parameters of VSM. Once the concurrence in terms of maximum displacement, between the experimental observations for SM and analytical values for VSM, is achieved, it may be perceived that SM and VSM are similar to each other. The amplitudes of the excitation at base, A_{be}, for which $A_e \approx D_m$, are selected and considered for further investigation into the performance of the SM-TSWDs coupling.
- Step 8: The optimized SM-TSWDs coupling (with water in the TSWDs) obtained from the free-vibration tests (as in Step 6) is subjected to the forced vibrations of magnitude determined from Step 7 through shake table tests. The sloshing mass of water is varied by increasing the number of

TSWDs. The reduced response of the SM due to its coupling with the TSWDs, under the dynamic loading, is used to arrive at the equivalent damping ratio ξ_e of the SM-TSWDs coupling by using Equation (3). The effectiveness E of the retrofitting system is determined from Equation (11) and then test-specific relations between ξ_e, E and μ are developed. The VSM is now analyzed with the damping ratio revised to ξ_e for the same loading as has been applied to the structure. The analytically determined displacement response reduction is then compared with the target response reduction. In the case of a major discrepancy between the two displacement values, the input value of ξ_e for the VSM is suitably revised to achieve the concurrence.

- Step 9: The dynamic similitude between SM, VSM and the structure is established and verified through Steps 1–8. The test observations may be extrapolated analytically for the real-life applications to the ES, considering that (i) the SM represents the structure and the SM together with the TSWDs represents the retrofitted structure and (ii) that the damping ratio of the structure has increased from ξ_s to ξ_e after retrofitting. The mass ratio required for the desired values of E and ξ_e is determined from the test-specific relationship obtained in Step 8. The sloshing mass required for the desired mass ratio is applied on the structure in the form of as many TSWDs as obtained by the arithmetical multiplication.

The above-described methodology bridges the gap between the analytical models and the real-life data for ES. This is explained in the following with the example of an existing structure.

DESCRIPTION OF EXISTING STRUCTURE

The existing structure considered in the present study is situated in Mumbai. It has been designed and executed in accordance with the prevalent code provisions (BIS, 2000). This structure is a residential building with a centrally located staircase, over which an overhead tank (OHT) is placed. All the columns are of 250×350 mm cross-section, except for the column B3, which is of 250×500 mm cross-section. A typical beam cross-section is of 230×400 mm dimensions along the X-axis and 230×450 mm dimensions along the Z-axis. The external and internal walls are of 230 and 115 mm thickness respectively and are constructed using burnt clay bricks with 1:4 cement sand mortar. The RC frame skeleton and structural floor plan of the building are shown in Figures 4 and 5, respectively.

The structure is structurally in a sound condition and shows no visible signs of distress or structural cracks. Hence, a damping of 3% has been assumed for the analysis (Newmark and Hall, 1978). The structure is modelled and analyzed by the software STAADPRO for the seismic conditions of the zone III (BIS, 2002). The salient features of the structure as determined analytically are given in Table 1**.** The frequency of the structure should lie in between the values for the two extreme conditions of full structural contribution and no structural contribution from the masonry. For the present study, the average value (i.e., 1.48 Hz along the Z-axis and 1.47 Hz along the X-axis) is considered. The retrofitting methodology is described in detail here with respect to the axis of symmetry along the Z-axis.

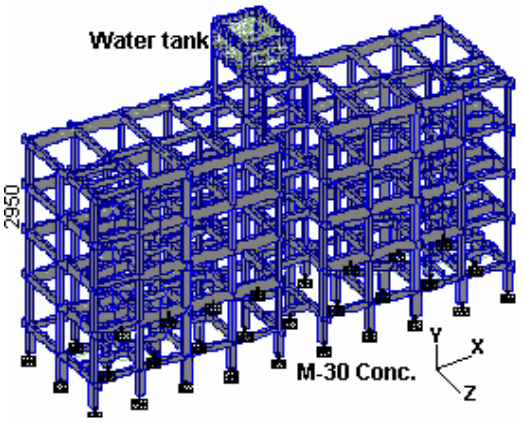

Fig. 4 RC frame of the existing structure considered

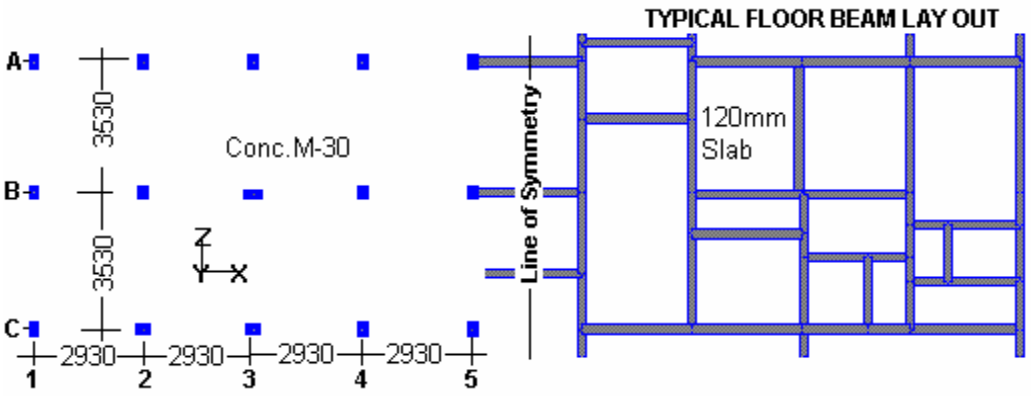

Fig. 5 Floor plan of the existing structure considered

Table 1: Salient Features of Existing Structure Considered

S. No.	Feature	Description
1	Mass of structure and mass participating in the first mode, m_s	1164000 kg; m_s = 885000 kg (for 76% mass participation in the first mode)
2	Damping ratio ξ_s	3% (Newmark and Hall, 1978)
3	Seismic zone	III (BIS, 2002)
4	First-mode frequency of the structure, ω_s, along the Z-axis	1.766 Hz (with masonry as the diagonal strut) 1.195 Hz (without a structural contribution of masonry)
	First-mode frequency of the structure, ω_s, along the X-axis	1.803 Hz (with masonry as the diagonal strut). 1.135 Hz (without a structural contribution of masonry)
5	Maximum displacement D_m	14.74 mm at the roof level along the Z-axis
		15.11 mm at the roof level along the X-axis
6	Permissible displacement D_p	11.05 mm at the roof level along the Z-axis.
		11.33 mm at the roof level along the X-axis.
7	Targeted effectiveness ratio E	25%

TSWDS FOR EXISTING STRUCTURE

For ω_d = 1.48 Hz and A_e = 11.05 mm, the TSWD parameters obtained from Equations (6)–(10) and Figure 3 are given in Table 2. Since Equation (9) gives slightly higher values of the sloshing mass, Equation (8) is considered for the present study.

Table 2: Parameters of Tuned Sloshing Water Dampers for Structure Considered

Size			Frequency along the Motion, ω_d (Hz)	Damping Ratio ξ_d (%)	Sloshing Mass m_d	
Length a (mm)	Depth h (mm)	Width b (mm)			Equation (8) (kg)	Equation (9) (kg)
284	80	145	1.479	18.13	2.1391	2.1749
220	40	145	1.481	20.77	0.9348	0.9538
182	25	145	1.479	23.00	0.5039	0.5149

SCALED MODEL OF EXISTING STRUCTURE, TSWD AND TEST SETUP

A 1:20 SM of the structure considered has been constructed with mild-steel (MS) wires, rods and plates (see Figure 6). The geometrical similarity in terms of the proportionality of plan dimensions,

elevations and floor heights between the structure and the SM is maintained. The self-weight of the SM is 39 kg. The imposed loads are applied in the form of rigidly attached lead blocks of 25 kg and MS blocks of different sizes. The symmetry of loading about the axis of symmetry is ensured in all the tests. The fine-tuning of the dynamic properties is accomplished by manipulating floor loads and their distribution. The displacement profile of the SM is also maintained comparable to that of the structure considered, for 3% inherent damping and under a similar loading.

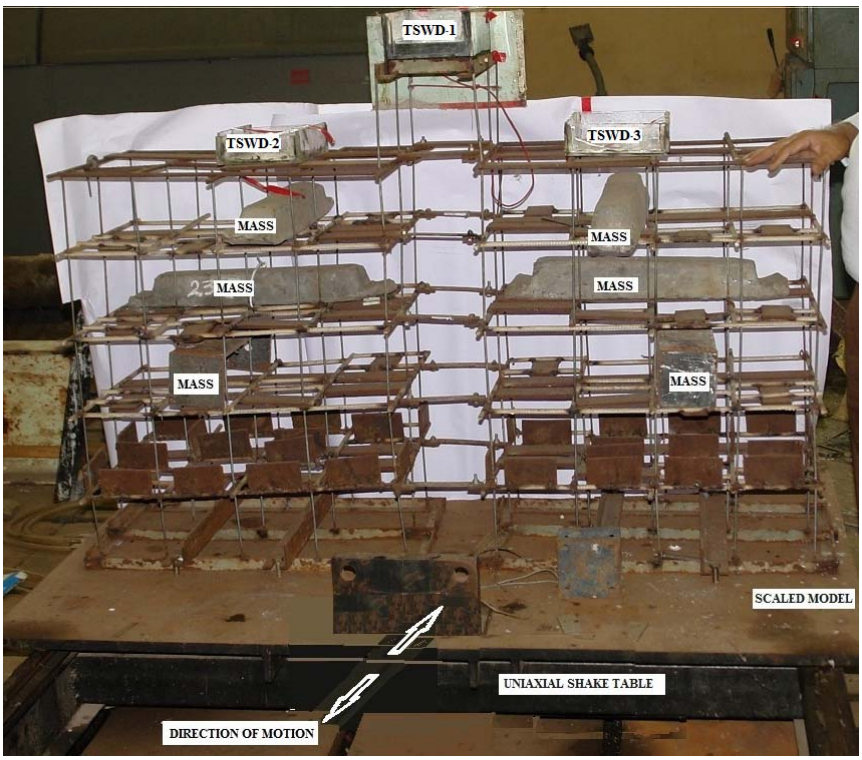

Fig. 6 Experimental setup with the TSWDs-mounted SM on the shake table

Three acrylic boxes, of internal dimensions 145×350 mm in plan and 100 mm depth, are rigidly attached with the SM to simulate the role of TSWDs. The box representing TSWD-1 is fixed on the four central columns extended from the main frame to simulate the OHT in the structure considered. The remaining boxes represent TSWD-2 and TSWD-3 and those are placed on the roof, one on each side of the axis of symmetry. All the three boxes are oriented in such a way that the 145-mm side is normal to the direction of vibration. The dimension of the TSWDs along the axis of vibration is varied by inserting a 145-mm acrylic sheet partition normal to the axis of vibration. The laser displacement sensor is fixed at the base of TSWD-1 to record the displacements during the tests. The scaled model and laboratory test setup are shown in Figure 6.

VIRTUAL SCALED MODEL OF EXISTING STRUCTURE

The VSM of the structure considered is developed in STAADPRO such that it is exactly similar to the SM (see Figure 7). The analytical values of the dynamic properties of the VSM are tabulated in Table 4 and 7.

EXPERIMENTAL VERIFICATION

The performance of the above retrofitting regime is verified by conducting laboratory simulations such that the retrofitted structure gives the assured performance during the real earthquakes. The test schedule is planned in four stages with free and forced vibrations, as described in Table 3. The free-vibration tests are conducted for verifying the consistency of the SM and TSWDs with respect to the analytical approach and for the assessment of the dynamic properties of the SM and TSWDs such that a suitable test regime is selected for experimental verification. The forced-vibration tests are planned and

conducted for simulating the coupled SM-TSWDs performance under the externally applied dynamic loading of resonant frequency as well as ground-motion time histories.

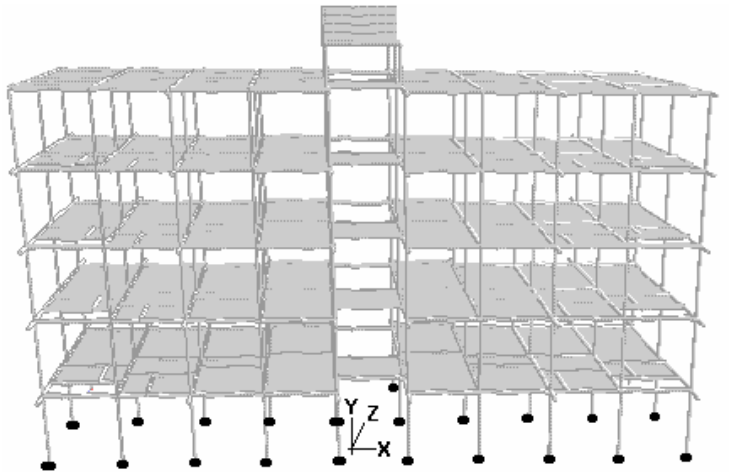

Fig. 7 Structural skeleton of the VSM

Table 3: Experimental Test Matrix

S. No.	Excitation Type	Purpose
1	Free vibration	On the bare SM, for the verification of consistency of SM and for the determination of frequency
2	Free vibration	On the SM-TSWDs system, for the determination of optimum TSWD parameters
3	Forced vibration (harmonic)	On the bare SM, for obtaining a suitable test regime and the range of base excitation amplitude A_{be}
		On the SM-TSWDs system, for the visualisation of response reduction due to TSWDs and the effect of mass ratio
4	Ground-motion time histories	For performance evaluation

FREE-VIBRATION TESTS

1. Verification and Behavioural Evaluation of Scaled Model

The bare SM (without water in TSWDs) is first subjected to an initial displacement of the order of 11 mm at the roof level and is then left free to vibrate. The vibration amplitudes are continuously recorded by the laser displacement sensor. The test is repeated, with different weight combinations at the floors, for the verification of the consistent behaviour of the SM and respective similitudes with the VSM. The SM under free vibration is observed over 25 cycles for the amplitude decay. The observed behaviour is then compared with the analytical results for the VSM as shown in Table 4.

Table 4: Results of Free-Vibration Tests on SMs

Test Model	Loading Description						Observed Frequency for SM (Hz)	Analytical Frequency for VSM	
	Ground Floor UDL (kg/m)	1st Floor (kg)	2nd Floor (kg)	3rd Floor (kg)	Roof (kg)	Total (kg)		Initial (Hz)	Modified (Hz)
SM-1	1.2	50	50	50	0	202	2.56	2.968	2.563
SM-2	1.2	50	50	50	50	252	2.41	2.881	2.390
SM-3	1.2	0	100	100	50	302	1.88	2.213	1.895
SM-4	1.2	118	118	118	7	413	1.76	2.047	1.759
SM-5	1.2	134	134	134	88	542	1.48	1.73	1.479

The free-vibration tests on the bare SM are primarily aimed to ascertain the consistency of the structural behaviour of the model under a dynamic loading. The observed frequencies of the SMs are less than the analytical frequencies of the VSM. This variance may be attributed to the nonuniformity in the sectional properties of the structural elements, imperfect fixity of the beam-column joints and the fixity of the model with the shake table. Hence, the VSM is arbitrarily modified by a 7.5% global reduction in the cross-sectional areas of all the structural elements and the modulus of elasticity of the material of the VSM. After these modifications, the analytical values show good concurrence with the observed values. The analytical values obtained after the modifications (in the VSM) are mentioned in the last column of Table 4. As the convergence of the observed and analytical values is similar for all the floor loading combinations and frequencies, the modification rule considered here is deemed adequate for the present model and test regime. Since the frequency of SM-5 is equal to that of the structure considered, the same is considered and designated as SM for further investigations.

The amplitude of vibration of the SM during the free-vibration tests is found to decay from 10.45 to 3.21 mm in 25 cycles. The damping ratio, as evaluated by the logarithmic decrement method, is 0.75% (see Figure 8). This value is consistent with the damping ratios adopted for the metal structures in elastic range (Adams and Askenazi, 1999). Further, the damping ratio of the SM for the first 10 cycles is 0.79% and for the last 10 cycles is 0.72%. The damping ratio of 0.75% is observed during the vibration amplitude of 8.5 to 7 mm. This suggests that the damping ratio is amplitude-dependent, and therefore, the representative amplitude considered in the present study is 70% of the maximum amplitude imparted.

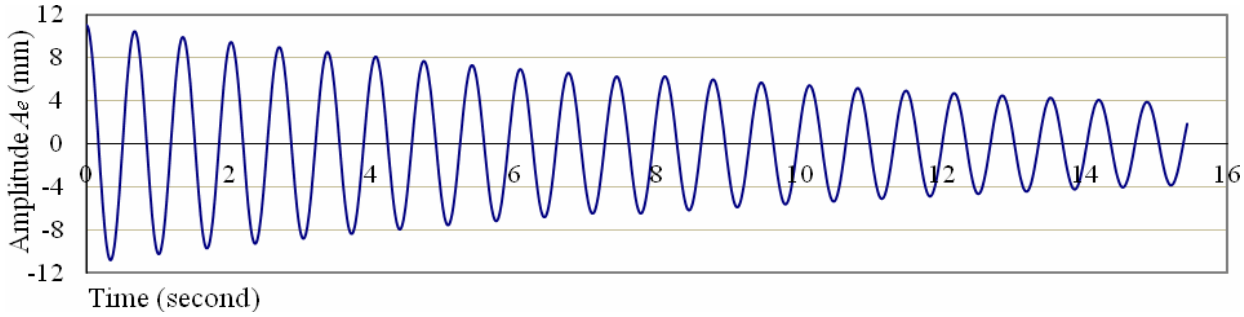

Fig. 8 Response time history during the free-vibration test on bare SM

2. Determination of Optimum TSWD Parameters in Coupling with SM

The coupled SM and TSWDs, with water only in TSWD-1, are subjected to free vibrations by giving an initial displacement of approximately 11 mm. The optimum length a of the TSWDs is searched over three analytically pre-determined depths of 80, 40 and 25 mm. This variation in length is implemented by inserting a 145-mm wide acrylic sheet partition normal to the direction of vibrations at different locations, with the depth of water remaining unchanged.

The displacement of the SM at the base of TSWD-1 is the excitation amplitude A_e for TSWD-1. The first set of the observations is recorded with 80 mm of water in TSWD-1. For every free-vibration observation, the effective damping ratio ξ_e of the SM-TSWDs system is determined by the logarithmic decrement method (see Table 5). The length of the TSWDs, at which the maximum value of ξ_e is obtained, is considered to be the optimum size of the TSWDs for perfect tuning with the SM, i.e., $\omega_s \approx \omega_d$.

For the SM-TSWDs system with 80-mm water depth, 280 mm is the optimum length of the TSWDs in the direction of vibrations. The significance of the mutual tuning of the structure and TSWDs may be substantiated here. Whereas in the tuned condition, 2.098 kg of water mass causes an increase in the effective damping from 0.75% to 1.5%, in the detuned condition with 350-mm length of the TSWDs, 2.82 kg of water mass is able to only achieve an effective damping ratio of 1.14% (see Table 5, Figure 9(a)). Similarly, the optimum lengths of TSWDs are obtained for the 40 and 25 mm of water depths (see Figures 9(b) and 9(c)).

Table 5: Optimum-Size Search for TSWD in Coupled Conditions with SM

Size			Effective Damping Ratio ξ_d (%)	Sloshing Mass m_d as per Equations (8)-(9) (kg)
Length a (mm)	Depth h (mm)	Width b (mm)		
350	80	145	1.14	2.822
320	80	145	1.30	2.512
290	80	145	1.46	2.201
260	80	145	1.40	1.890
280	80	145	1.50	2.098
270	80	145	1.47	1.994

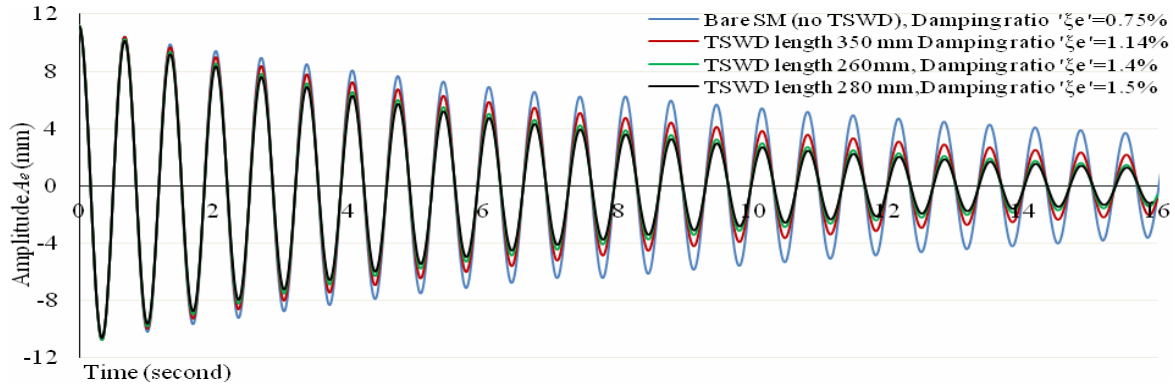

(a)

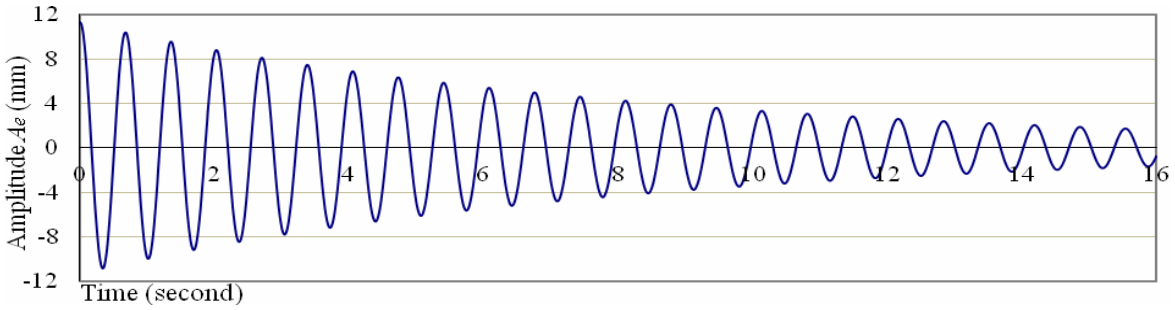

(b)

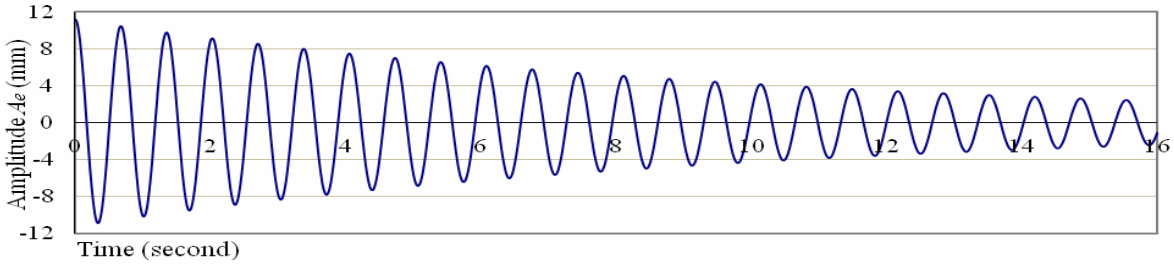

(c)

Fig. 9 (a) Determination of effective damping ratio ξ_e of SM-TSWDs system with 80-mm water depth; (b) Determination of optimum effective damping ratio ξ_e of SM-TWDSs system with 40-mm water depth, (c) Determination of optimum effective damping ratio ξ_e of SM-TSWDs system with 25-mm water depth

The results of the free-vibration tests show the effectiveness of the SM-TSWDs system, as an increase is observed in the effective damping ratio of the system for all sizes of TSWDs. The

dimensions and effective damping ratio of the TSWDs, as obtained experimentally, are tabulated in Table 6. The effective damping ratio ξ_e of the SM-TSWDs system is sensitive to the tuning ratio $f = \omega_d / \omega_s$. In turn, ω_d is sensitive to the amplitude of excitation, $A_{e,\max}$. Thus, the amplitude of excitation of TSWDs is an important parameter for the design of retrofitting system.

Two additional sets of data for the relevant TSWD parameters are generated analytically (by using Equations (2)–(9) and Figure 3) for $A_{e,\max}$ and for 70% of $A_{e,\max}$ for each TSWD. The analytical values are compared with the experimentally obtained values in Table 6. It is seen that the analytical values of ξ_e obtained with 70% of $A_{e,\max}$ are in good concurrence with the observed values. The spread of experimentally obtained values of ξ_e with respect to mass ratio suggests an almost linear relationship between them in the perfectly tuned condition (see Figure 10).

Table 6: Experimentally and Analytically Obtained TSWD Parameters

S. No.	TSWD Ident.	Experimental Values			Analytically Derived Values						
						At $A_{e,\max}$			At 70% of $A_{e,\max}$		
		Length a (mm)	Depth h (mm)	Effect. Damping Ratio ξ_e (%)	Sloshing Mass m_d Eq. (9) (kg)	ω_d Eqs. (7) (Hz)	ξ_d Fig. 3 (%)	ξ_e Eq. (4) (%)	ω_d Eqs. (7) (Hz)	ξ_d Fig. 3 (%)	ξ_e Eq. (4) (%)
1	$TSWD_{80}$	350	80	1.14	2.822	1.210	16.25	1.14	1.199	13.51	1.13
2	$TSWD_{80}$	280	80	1.50	2.098	1.500	18.27	1.33	1.446	15.16	1.44
3	$TSWD_{40}$	210	40	1.29	1.388	1.553	21.29	1.06	1.485	17.62	1.12
4	$TSWD_{25}$	174	25	1.02	0.952	1.552	23.57	0.93	1.484	19.46	0.98

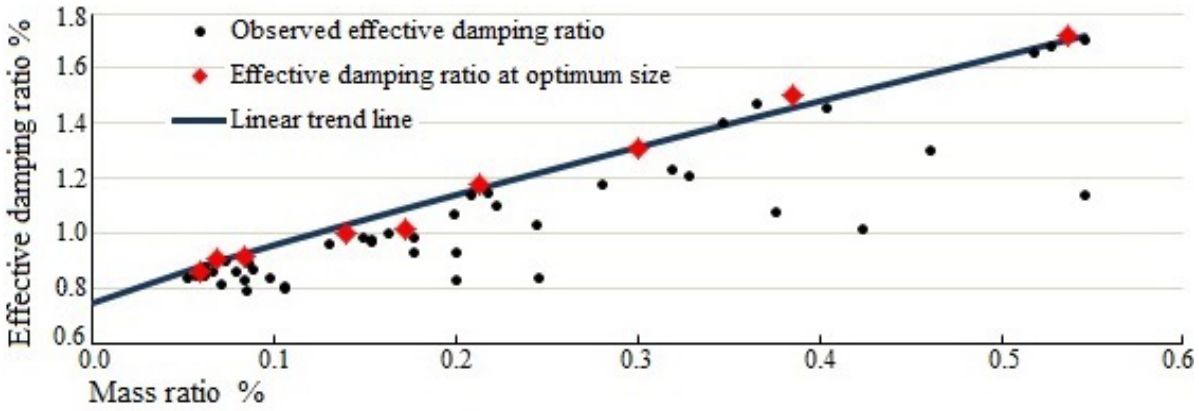

Fig. 10 Variation of experimentally determined effective damping ratio with mass ratio under free vibrations

FORCED-VIBRATION TESTS

1. SM Subjected to Harmonic Excitation (Bare Test)

The dynamic properties of the SM are already assessed by the free-vibration tests as discussed above. The SM with no water in the TSWDs is now subjected to sinusoidal excitations at the resonant frequency of 1.48 Hz. These tests are designated as bare tests. Five sets of forced-vibration tests with varying amplitudes of sinusoidal excitations, A_{be}, at the base of SM are conducted. The amplitude A_{be} is increased from 0.25 to 1.25 mm in the incremental steps of 0.25 mm. The performance of the bare SM is observed and recoded for 50 cycles in each set. The displacements observed at the level of TSWD-1 and the evaluated damping ratios of SM are given in Table 7.

Table 7: Comparison of Performances of SM and VSM under Forced Vibrations

S. No.	Amplitude of Excitation at Base, A_{be} (mm)	Experimental Observations for SM		Analytical Values for VSM	
		Displacement (mm)	Damping Ratio (%)	Initial (mm)	Modified (mm)
1	0.25	4.94	2.53	4.42	4.901
2	0.5	9.23	2.71	8.51	9.358
3	0.75	12.24	3.06	11.46	12.56
4	1	15.75	3.17	14.39	15.862
5	1.25	17.75	3.52	16.21	17.979

The VSM is also analyzed for the observed damping ratios and for the same excitations as applied to the SM. The displacements thus obtained are tabulated (see Columns 4 and 5 of Table 7). The modification rule applied to the VSM for the free-vibration tests is thus substantiated.

2. SM-TSWDs System Subjected to Harmonic Excitations

The TSWD parameters are amplitude dependent, implying different values of these parameters for different vibration amplitudes. The maximum vibration amplitude $A_{e,\max}$ of the TSWDs is same as the maximum structural displacement D_m at the TSWD locations. The maximum displacement of the structure considered is 14.74 mm. Maximum displacements of the same order are observed in the bare SM for the amplitudes of excitation at the base, A_{be}, equal to 0.75 and 1.0 mm. The effects of the retrofitting performance of the TSWDs on the SM are, therefore, studied for these sinusoidal base excitations.

Each acrylic box is converted into a TSWD of 145-mm width (i.e., b measured normal to the direction of excitation). The length of the TSWDs is fixed by inserting a 4-mm thick acrylic sheet. The experimental observations are taken with the combination of $TSWD_{80}$ and $TSWD_{25}$ in the case of 9 mass ratios varying from 0.177 to 2.34% (see Table 8). The effectiveness of the TSWDs on the performance of the SM is evident from these results.

Table 8: Performance of SM-TSWDs System under Harmonic Excitation

Test No.	Mass Ratio μ (%)	Maximum Displacement (mm)	Effective Damping Ratio (%)			Maximum Displacement (mm)	Effective Damping Ratio (%)		
			Observed	Analytical			Observed	Analytical	
				At $A_{e,\max}$	At 70% of $A_{e,\max}$			At $A_{e,\max}$	At 70% of $A_{e,\max}$
		Amplitude of Excitation at Base, A_{be} = 0.75 mm				Amplitude of Excitation at Base, A_{be} = 1.0 mm			
1	0	12.24	3.06	Bare test		15.75	3.17	Bare test	
2	0.177	11.2	3.35	3.22	3.27	14.25	3.51	3.3	3.34
3	0.354	10.26	3.66	3.38	3.51	13.23	3.78	3.43	3.52
4	0.53	9.38	4.00	3.55	3.77	12.2	4.1	3.57	3.7
5	0.757	8.67	4.33	3.98	4.28	11.39	4.39	3.9	4.18
6	0.991	8.02	4.68	4.31	4.67	10.57	4.73	4.18	4.54
7	1.228	7.55	4.97	4.54	4.86	9.98	5.01	4.3	4.65
8	1.56	6.47	5.58	4.99	5.36	9.26	5.4	4.82	5.16
9	2.34	6.05	6.42	5.97	6.51	8.06	6.42	5.71	6.22

As has been done for the free-vibration tests, two additional sets of data are generated analytically for the effective damping ratio ξ_e in the cases of $A_{e,\max}$ and 70% of $A_{e,\max}$ for each mass ratio and are tabulated in Table 8. It may be observed that the inference of free-vibration tests that analytical values for 70% of $A_{e,\max}$ are closer to the experimental values of ξ_e is substantiated. Thus, it follows that the

characteristic parameters of TSWDs should be analytically evaluated for 70% of $A_{e,\max}$. Further, the experimentally observed effective damping ratio exhibits a relationship with the mass ratio as shown in Figure 11. This relationship may be expressed empirically as

$$\xi_e = \xi_s + \left(5/\xi_s\right)\mu^{0.9} \tag{12}$$

where the constant of 5 is derived from the fact that the damping ratio of 5% is the standard reference point in all the codal treatments (Nawrotzki, 2005).

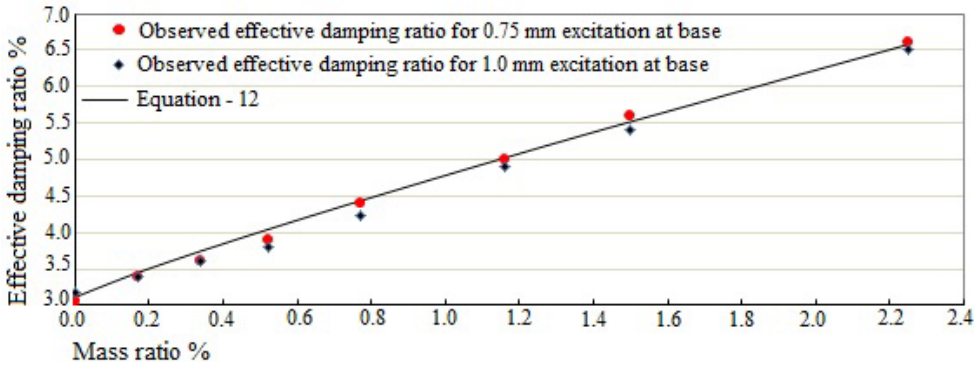

Fig. 11 Variation of experimentally observed effective damping ratio with mass ratio

For the base excitation amplitude A_{be} of 0.75 and 1.0 mm, the behaviour of SM with and without TSWDs is plotted for the mass ratio of 1.228%. A more than 35% reduction in the maximum cyclic displacement of SM is observed as shown in Figures 12(a) and 12(b).

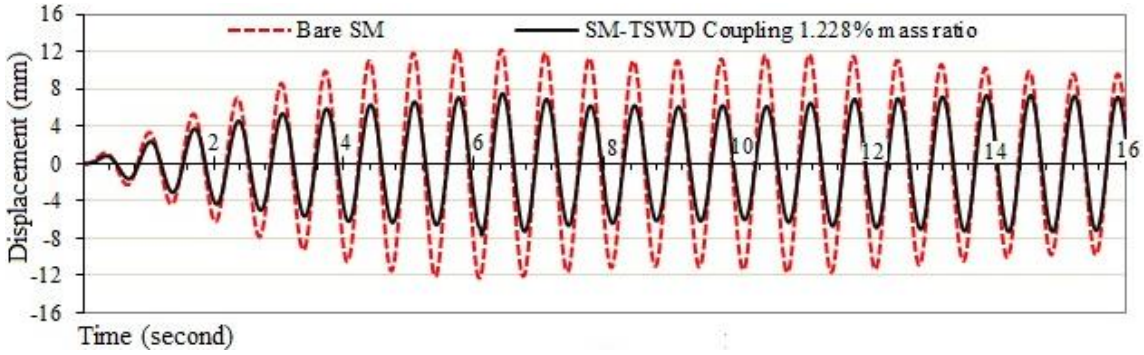

(a)

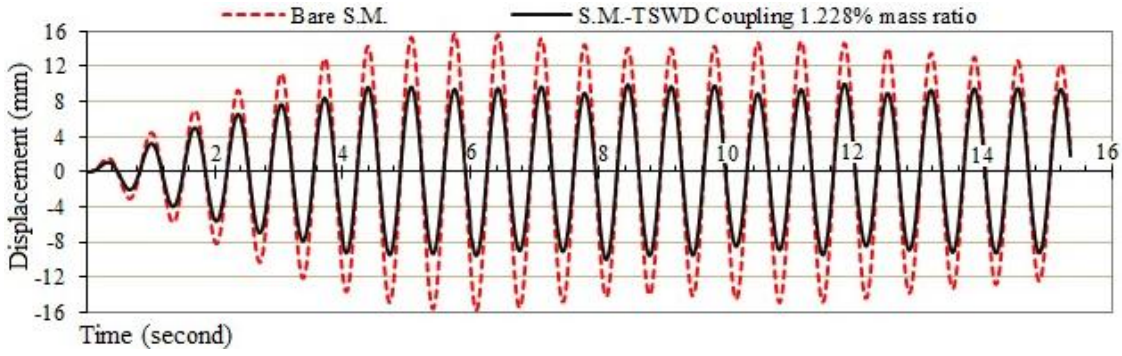

(b)

Fig. 12 Performance of SM-TSWDs system under harmonic excitation: (a) response reduction of 38.7% for the excitation amplitude at base A_{be} = 0.75 mm; (b) response reduction of 36.5% for the excitation amplitude at base A_{be} = 1.0 mm

3. SM-TSWDs System Subjected to Ground-Motion Time History

The performance of the retrofitting system is further substantiated with respect to ground-motion time histories. The SM is subjected to the ground motion recorded during the 1940 El Centro earthquake as in Chopra (1995) and a time-history compatible with the response spectrum of the IS 1893 code (BIS, 2002). The maximum displacement observations of the bare SM with three $TSWD_{80}$s are recorded for the mass ratio of 1.228%. The corresponding vibration profiles are plotted in Figures 13(a)–13(c). It may be observed that the effectiveness of the retrofitting system used is less as compared to that under the sinusoidal excitations. This may be attributed to the fact that the TSWDs were designed for the excitation amplitude of 11.05 mm, which may not be the same as that experienced by the TSWDs under the ground-motion histories considered here.

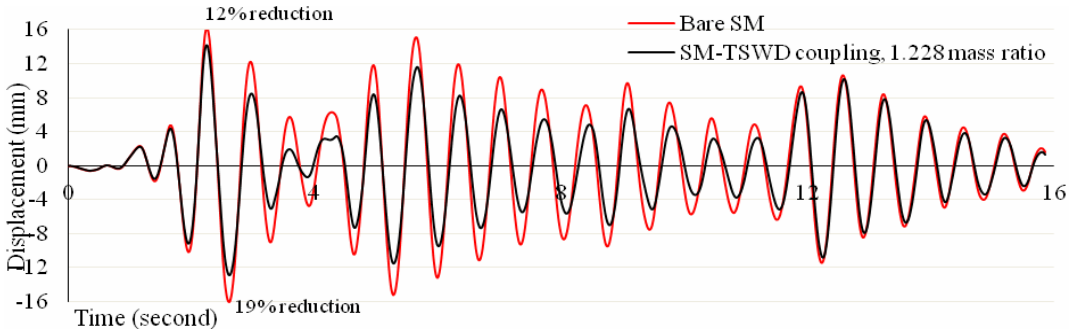

(a)

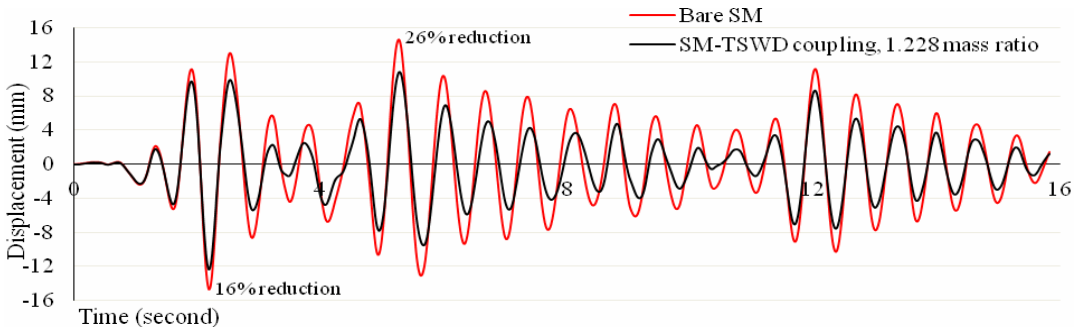

(b)

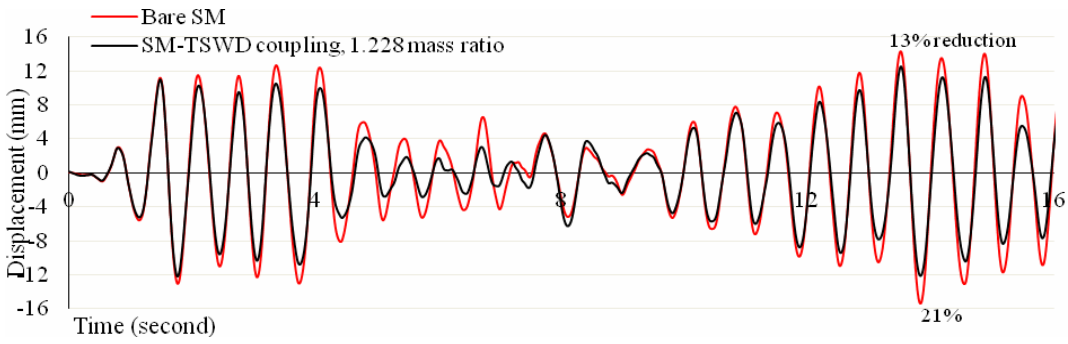

(c)

Fig. 13 Performance of SM-TSWDs system under ground motions: (a) EW-component of El Centro motion; (b) NS component of El Centro motion; (c) IS-1893 compatible time history

4. SM and TSWD Parameters along X-Axis

The above-described test matrix and analytical procedures are repeated with the SM oriented by 90° such that the X-axis of the SM is parallel to the direction of vibrations. The acrylic boxes used as

TSWDs are of 280×350 mm in plan and 100 mm in depth, with the 280-mm side oriented normal to the axis of vibration. The properties of the SM and TSWDs thus obtained are as follows:

- mass of SM: 502 kg
- frequency: 1.47 Hz (as obtained from the free-vibration tests, modification rule of 7.5% global reduction in the cross-sectional area and modulus of elasticity, and verified with VSM)
- damping ratio: 3.25% (under forced vibration with the sinusoidal excitation amplitude at the base, A_{be} = 1.0 mm)
- length a of $TSWD_{80}$: 280 mm
- sloshing mass in $TSWD_{80}$: 4.05 kg

It is seen that the experimental observations substantiate the concept and the modification rule considered. Further, $TSWD_{80}$ with 280×280-mm plan size and 80-mm depth has effectiveness along both the principal axes of the SM. The total mass of the water contained in the $TSWD_{80}$ is 6.27 kg.

EFFECTIVENESS OF SM-TSWD COUPLING

The relationship between the mass ratio and effectiveness is nonlinear and depends on all the parameters already included in Equations (2)–(5) (i.e., f, μ, β, ξ_s and ξ_d). From the experimental data tabulated in Table 8, a plot is developed between E and μ (see Figure 14). This shows that the effectiveness of the retrofitting system considered increases with an increase in the mass ratio. For the present SM-TSWD coupling, therefore, the E and μ relationship may be approximated by a linear equation as

$$E = K\mu \tag{13}$$

This equation may be considered as a model-specific approximate expression for the nonlinear relationship existing between effectiveness and mass ratio. The factor K here represents a gross value for the cumulative effects of all the mutually interactive parameters of the structure and TSWDs. It may vary for different systems and structure-TSWDs combinations. Equation (13) may be used to obtain a quick preliminary estimate of the mass ratio for desired effectiveness. The so-estimated mass ratio leads to the effective damping ratio of the retrofitted structure through Equation (12). This value of effective damping is then checked analytically for the desired response reduction.

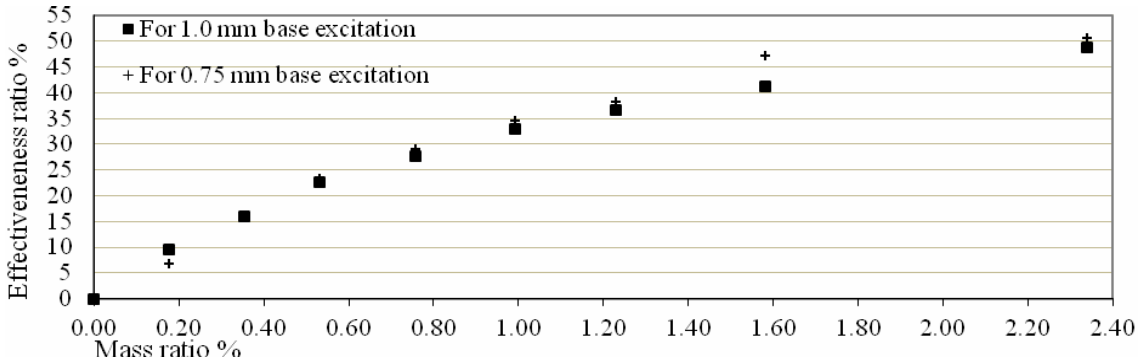

Fig. 14 Observed effectiveness of the SM-TSWD coupling for varying mass ratio

APPLICATION OF THE TSWD RETROFITTING SYSTEM TO ES

The TSWD-based retrofitting concept as discussed above is directly applicable to the existing structures for improving their seismic performance (Reddy et al., 2008). For example, in the case of the structure considered above, the structure has already been analyzed (see Table 1) and a SM having dynamic similitude with this has already been tested and visualized in the laboratory. The design of a retrofitting system for this structure thus becomes a simple arithmetical iterative exercise. We conduct this exercise for a desired effectiveness ratio of 25% as given below.

1. 1st Iteration

For the SM-TSWDs system experimentally investigated, the value of K, as obtained from Figure 14, is 25. Equation (13) thus gives the required mass ratio μ for 25% effectiveness ratio E as 1.0%. For this mass ratio, Equation (12) gives the estimated value of effective damping ratio ξ_e as 4.72%. Thus, on adopting the TSWD-based retrofitting scheme, the effective damping ratio of the structure is deemed to increase to 4.72%, as against the initial 3% for the unretrofitted state. The VSM is now analyzed for the increased damping ratio of 4.72% and the resultant maximum displacement is obtained as 10.48 mm along the Z-axis, corresponding to the effectiveness ratio achieved as 28.9%. The structure considered above is also analyzed with the increased damping ratio of 4.72% and the maximum displacement obtained is 12.28 mm along the Z-axis. Thus, the effectiveness ratio achieved is only 16.7%, as against the targeted value of 25%. This may be attributed to the fact that the total mass of the structure is not participating in the first mode of vibration.

It may be inferred from the above that the value K = 25, as determined for the SM-TSWDs system, is not applicable to the retrofitted structure and has to be revised, thus leading to the 2nd iteration.

2. 2nd Iteration

The retrofitting regime as considered above is redesigned with an increase in the damping mass to achieve the desired effectiveness. Since the effective ratio achieved is 16.7% for the mass ratio of 1.0%, the factor K is revised to the value of 16.7 on using Equation (13). This leads to the required mass ratio μ of 1.5% and effective damping ratio ξ_e of 5.4%. With this (increased) damping ratio, the analytically determined maximum displacement for the structure is 11.03 mm along the Z-axis and 11.28 mm along the X-axis, which is less than the targeted reduced response. The corresponding sloshing mass M_d to be contained in the TSWDs is $m_s\mu$ = 13275 kg and thus the number of TSWDs required becomes N = 3278 units (on using Equation (5)). It may be mentioned that the seismic response of the structure considered may be reduced further by increasing the sloshing mass.

3. Execution Scheme

The total mass of water contained in one unit of $TSWD_{80}$ is 6.27 kg and the sloshing mass of water in each unit is 4.05 kg. As discussed above, a total of 3278 $TSWD_{80}$s are to be provided for achieving the required mass ratio. To this end, the existing water tank may be converted to 100 TSWDs of 280×280-mm plan size by inserting 1-mm thick GI partitions (see Figure 15(a)). The remaining 3178 TSWDs of 280×280×130-mm size may be provided in four clusters at the roof of the structure. Each cluster contains 800 $TSWD_{80}$ in five tiers and each tier contains 4 rows of 40 $TSWD_{80}$. These clusters of TSWDs may be fabricated in GI sheet, as shown in Figures 15(b) and 15(c).

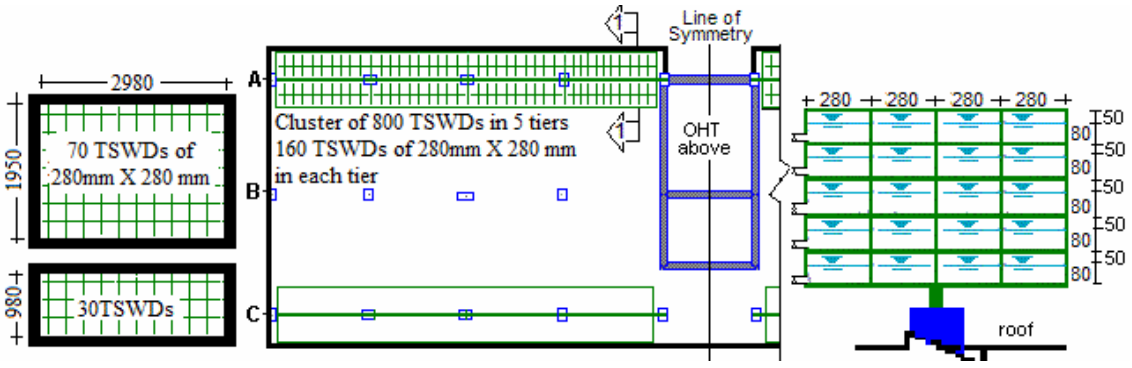

(a) (b) (c)

Fig. 15 Execution scheme of TSWD-based retrofitting system on the existing system considered: (a) OHT converted as TSWDs; (b) plan at roof level; (c) Section 1-1

The increase in structural mass due to the provision of additional 3200 units of TSWDs will be approximately equal to 20070 kg. The mass of the 150-mm thick and 1050-mm high parapet wall on the

roof is 22600 kg and thus the increase in structural mass (due to the provision of TSWDs) may be compensated by replacing the masonry parapet by an MS-piped railing. Thus, a sloshing mass of 13365 kg contained in 3300 TSWDs is accommodated on the roof, which will act as $TSWD_{80}$ under the seismic excitations, without causing any architectural, structural or occupancy interference with the structure considered.

Similar multi-layered TSWDs are already installed and performing well against the wind excitations in tall structures, such as Nagasaki airport tower, Yokohoma marine tower, Shin-Yokohoma prince hotel, and Tokyo international airport tower (Tamura et al., 1995). The effectiveness of the retrofitting scheme for an earthquake loading has been already established through experimental simulations with different sizes of TSWDs having same natural frequency. It has also been demonstrated that for a given tuning ratio, retrofitting performance is dependent on the mass ratio. Thus, the performance of the retrofitting regime under an earthquake loading is assured by the provision of adequate sloshing mass in a cluster of multi-layered TSWDs.

4. Comparison with TLCD Proposition

It is evident from Figure 15 that even after the incorporation of TSWD-based retrofitting regime in the structure considered, its roof is available for the other utilities. For a comparable performance with a TLCD-based retrofitting regime, it may be mentioned that based on the available design methods (Sadek et al., 1996), 44640 U-shaped TLCDs of 40-mm internal diameter, 188-mm horizontal length and 40-mm vertical arm with orifice opening ratio of 0.75 would be required along each principal axis. The provision of 89280 TLCDs on roof will be highly cumbersome. Further, TLCDs will be ineffective in the directions other than the principal axes.

CONCLUDING REMARKS

This study has focussed on the coupled behaviour of the ES retrofitted with TSWDs for their best performance under various dynamic excitations. The interaction of ES with TSWDs has been investigated by employing a 'hardware interactive soft path' method. This method involves an intermittent use of theoretical formulations, their experimental verification, and the development of a case-specific application rule. This method compensates for the real-life field data by simulated experimental investigations.

Experiments have been conducted to investigate the performance of the SM-TSWD coupling. The accuracy of the empirical relations proposed by previous researchers has been checked for the tuned condition by varying other parameters (i.e., different types of loading, levels of excitation frequency, amplitudes of excitation and mass ratios). For the excitation amplitudes equivalent to 70% of the maximum amplitude, the convergence of the experimental results has been very good with the empirical relations proposed by previous researchers. The modification rule of 70% vibration amplitude has been observed in the free-vibration tests and validated through the forced-vibration tests.

A structure-specific relationship exists between the mass ratio and effectiveness of the proposed retrofitting regime. For the SM-TSWD coupling considered here, this is represented by Equation (13) with K = 25. The value of K may be modified for other combinations (e.g., K = 16.7 for the ES-TSWD coupling).

It has been observed that TSWDs are more effective for the structures with low damping ratios. This phenomenon has been encapsulated in Equation (12). The effective damping ratio ξ_e in this equation has been derived from the decreased structural displacements due to the incorporation of TSWDs. The TSWDs have been observed to be effective from the start of the dynamic motion without any time lag (see Figures 12 and 13), thus ensuring a real-time structural response control.

The equations and plots developed through the shake table tests have been applied for developing a retrofitting regime of an existing structure. It has been seen that the effective damping of the structure considered increases from 3 to 5.4% without any loss of stiffness. Further, a seismic response reduction of 25% with 1.5% sloshing mass is achievable for the structure considered.

The TSWDs to be attached to the ES have been tested for their retrofitting effect on a SM having the dynamic similitude of the ES, for all types of dynamic excitations. The observed effectiveness of the TSWDs in reducing the response of SM against forced vibrations is also valid for the real-life structures with comparable dynamic similitudes. In effect, the retrofitting system tested in the laboratory has been

amplified manifold for its effectiveness on a real-life structure, thus providing a very high degree of performance assurance. The structure considered in this study is representative of the existing building stock. Hence, most of the medium-height existing structures, designed and constructed with the working stress principles, may be retrofitted with TSWDs for safety against the likely earthquake forces.

The proposed TSWD-based method of seismic retrofitting for the existing structures addresses the serviceability, safety and durability concerns. This method is easy to execute, environmentally sustainable, and cost effective, and this ensures all-time preparedness against earthquakes without requiring any post-retrofitting maintenance.

REFERENCES

1. Abramson, H.N. (editor) (1966). "The Dynamic Behavior of Liquids in Moving Containers, with Applications to Space Vehicle Technology", Report NASA SP-106 Prepared by the Southwest Research Institute, National Aeronautics and Space Administration, Washington, DC, U.S.A.
2. Adams, V. and Askenazi, A. (1999). "Building Better Products with Finite Element Analysis", OnWord Press, Santa Fe, U.S.A.
3. BIS (2000). "IS 456: 2000—Indian Standard Plain and Reinforced Concrete—Code of Practice (Fourth Revision)", Bureau of Indian Standards, New Delhi.
4. BIS (2002). "IS 1893 (Part 1): 2002—Indian Standard Criteria for Earthquake Resistant Design of Structures, Part 1: General Provisions and Buildings (Fifth Revision)", Bureau of Indian Standards, New Delhi.
5. Chopra, A.K. (1995). "Dynamics of Structures: Theory and Applications to Earthquake Engineering", Prentice-Hall, Inc., Englewood Cliffs, U.S.A.
6. Connor, J.J. (2003). "Introduction to Structural Motion Control", Prentice Hall, Englewood Cliffs, U.S.A.
7. Den Hartog, J.P. (1962). "Mechanical Vibrations", McGraw-Hill, New York, U.S.A.
8. Frahm, H.H. (1911). "Results of Trials of the Anti-rolling Tanks At Sea", Journal of the American Society for Naval Engineers, Vol. 23, No. 2, pp. 571–597.
9. Graham, E.W. and Rodriguez, A.M. (1952). "The Characteristics of Fuel Motion Which Affect Airplane Dynamics", Journal of Applied Mechanics, ASME, Vol. 19, No. 3, pp. 381–388.
10. Hassan, M. (2010). "A Numerical Study of the Performance of Tuned Liquid Dampers", M.S. Thesis, Department of Mechanical Engineering, McMaster University, Hamilton, Canada.
11. Housner, G.W. (1963). "The Dynamic Behavior of Water Tanks", Bulletin of the Seismological Society of America, Vol. 53, No. 2, pp. 381–387.
12. Kareem, A. and Sun, W.J. (1987). "Stochastic Response of Structures with Fluid Containing Appendages", Journal of Sound and Vibration, Vol. 119, No. 3, pp. 389–408.
13. Langhaar, H.L. (1951). "Dimensional Analysis and Theory of Models", John Wiley & Sons, Inc., New York, U.S.A.
14. Malekghasemi, H. and Mercan, O. (2011). "Experimental and Analytical Investigations of Rectangular Tuned Liquid Dampers (TLDs)", RCI Report No. 2011-02, Department of Civil Engineering, University of Toronto, Toronto, Canada.
15. Modi, V.J. and Welt, F. (1987). "Vibration Control Using Nutation Dampers", Proceedings of the International Conference on Flow Induced Vibrations, Bowness-on-Windermere, U.K., pp. 369–376.
16. Nawrotzki, P. (2005). "Visco-elastic Devices for the Seismic Control of Machinery, Equipment and Buildings", Proceedings of the 9th World Seminar on Seismic Isolation, Energy Dissipation and Active Vibration Control of Structures, Kobe, Japan (on CD).
17. Newmark, N.M. and Hall, W.J. (1978). "Development of Criteria for Seismic Review of Nuclear Power Plants", Report NUREG/CR-0098, U.S. Nuclear Regulatory Commission, Washington, D.C., U.S.A.

18. Rai, N.K., Reddy, G.R. and Venkatraj, V. (2010). "Seismic Retrofitting of Existing Structures: Over Head Tank as TSWD", Proceedings of the 14th Symposium on Earthquake Engineering, Roorkee, Vol. 2, pp. 1294–1305.
19. Rai, N.K., Reddy, G.R. and Venkatraj, V. (2011). "Technical Note: Effectiveness of Multiple TSWD for Seismic Response Control of Masonry Infilled RC Framed Structure", ISET Journal of Earthquake Technology, Vol. 48, No. 2-4, pp. 85–103.
20. Reddy, G.R., Parulekar, Y.M., Dubey, P.N., Sharma, A., Vaity, K.N., Ravi Kiran, A., Agrawal, M.K., Vaze, K.K., Ghosh, A.K. and Kushwaha, H.S. (2008). "Studies on Response of Structures, Equipment and Piping Systems to Earthquake and Its Mitigation", BARC Newsletter, No. 290, pp. 15–30.
21. Sadek, F., Mohraz, B. and Lew, H.S. (1996). "Single and Multiple Tuned Liquid Column Dampers for Seismic applications", Report NISTIR 5920, National Institute of Standards and Technology, Gaithersburg, U.S.A.
22. Sakai, F., Takaeda, S. and Tamaki, T. (1989). "Tuned Liquid Column Damper—New Type Device for Suppression of Building Vibrations", Proceedings of the International Conference on Highrise Buildings, Nanjing, China, Vol. 2, pp. 926–931.
23. Sharma, A., Reddy, G.R. and Vaze, K.K. (2012). "Shake Table Tests on a Non-seismically Detailed RC Frame Structure", Structural Engineering and Mechanics, Vol. 41, No. 1, pp. 1–24.
24. Sun, L.M., Fujino, Y., Chaiseri, P. and Pacheco, M. (1995). "The Properties of Tuned Liquid Dampers Using a TMD Analogy", Earthquake Engineering & Structural Dynamics, Vol. 24, No. 7, pp. 967–976.
25. Tait, M.J. (2008). "Modelling and Preliminary Design of a Structure-TLD System", Engineering Structures, Vol. 30, No. 10, pp. 2644–2655.
26. Tamura, Y., Fujii, K., Ohtsuki, T., Wakahara, T. and Kohsaka, R. (1995). "Effectiveness of Tuned Liquid Dampers under Wind Excitation", Engineering Structures, Vol. 17, No. 9, pp. 609–621.
27. Warburton, G.B. (1981). "Optimum Absorber Parameters for Minimizing Vibration Response", Earthquake Engineering & Structural Dynamics, Vol. 9, No. 3, pp. 251–262.
28. Yalla, S.K. (2001). "Liquid Dampers for Mitigation of Structural Response: Theoretical Development and Experimental Validation", Ph.D. Dissertation, Department of Civil Engineering and Geological Sciences, University of Notre Dame, Notre Dame, U.S.A.
29. Yu, J.K. (1997). "Nonlinear Characteristics of Tuned Liquid Dampers", Ph.D. Dissertation, Department of Civil & Environmental Engineering, University of Washington, Seattle, U.S.A.